Substorm inner plasma sheet particle reduction

L. R. Lyons,[1] C.-P. Wang,[1] T. Nagai,[2] T. Mukai,[3] Y. Saito,[3] and J. C. Samson[4]

Received 1 August 2003; revised 10 September 2003; accepted 24 September 2003; published 9 December 2003.

[1] Geotail measurements from within the equatorial inner plasma sheet at r ~ 10–13 R_E are used to show that a reduction in equatorial plasma pressure within the current wedge is a general feature of substorms and that this decrease is simultaneous with the well-known expansion phase increase in energetic particle fluxes. The decrease in pressure is found to be due to a decrease in particle fluxes at lower energies that gives a significant decrease in plasma density. We also find that when viewed as a function of the adiabatic energy invariant for the plasma sheet λ, there is a reduction in the number of particles for all λ despite the enhancements seen when energetic particle fluxes are viewed at fixed particle energy. These observations demonstrate that the expansion phase is associated with a significant reduction in flux tube content of particles within the current wedge and that this reduction leads to the expansion-phase reduction in equatorial plasma pressure and cross-tail current. *INDEX TERMS:* 2788 Magnetospheric Physics: Storms and substorms; 2764 Magnetospheric Physics: Plasma sheet; 2704 Magnetospheric Physics: Auroral phenomena (2407); 2431 Ionosphere: Ionosphere/magnetosphere interactions (2736); *KEYWORDS:* substorms, plasma sheet, geomagnetic tail, magnetosphere-ionosphere coupling, aurora

Citation: Lyons, L. R., C.-P. Wang, T. Nagai, T. Mukai, Y. Saito, and J. C. Samson, Substorm inner plasma sheet particle reduction, *J. Geophys. Res.*, *108*(A12), 1426, doi:10.1029/2003JA010177, 2003.

1. Introduction

[2] The substorm expansion-phase occurs in association with a region of reduced cross-tail current that is connected to the ionosphere by field-aligned currents. These field-aligned currents are directed out of (into) the ionosphere on the dusk (dawn) side of the region of cross-tail current reduction and close in the ionosphere via the westward electrojet that forms at expansion phase onset. The entire system consisting of the region of reduced cross-tail current, field-aligned currents, and the auroral electrojet is referred to as the "substorm current wedge" [e.g., *McPherron et al.*, 1973; *Moore et al.*, 1981], and this current wedge is known to initiate within the inner plasma sheet [*Jacquey et al.*, 1991, 1993; *Samson et al.*, 1992; *Ohtani et al.*, 1992]. Understanding how the current wedge is formed is critical to understanding the substorm expansion phase.

[3] Under the assumption of pressure balance, the magnitude of the cross-tail current per unit of distance down the tail is proportional to $P_{eq}^{1/2}$, where P_{eq} is the equatorial plasma pressure within the nightside plasma sheet. (This pressure balance assumption is not strictly valid when the component of magnetic field normal to the current sheet is significant [e.g., *Petrukovich et al.*, 1999a], but it is generally a useful approximation.) Thus the reduction in cross-tail current within the current wedge should be associated with a decrease in P_{eq}. This pressure decrease should occur despite the increase in energetic particle fluxes that occurs within the inner plasma sheet as the magnetic field dipolarizes within the current wedge. Also, this pressure decrease would represent a significant decrease in $P_{eq}\mathcal{V}^{5/3}$, where $\mathcal{V} = \int ds/B$ is the flux tube volume per unit magnetic flux, since $\mathcal{V}$ decreases as the magnetic field dipolarizes.

[4] It is known that the lobe magnetic field and the tail total (magnetic plus plasma) pressure decrease at substorm onset [*Caan et al.*, 1975; *Miyashita et al.*, 2000], implying by pressure balance that the equatorial plasma pressure does decrease as discussed above. However, there have been very few direct measurements of the change in equatorial plasma pressure within the near-Earth plasma sheet during substorms. This is in part due to the limited number of spacecraft measurements obtained within the inner plasma sheet region of substorm onset and to the low probability of a spacecraft being near the equatorial plane (defined as the center of the cross-tail current sheet) before and after an onset. The only direct measurements of which we are aware are one example at geosynchronous orbit [*Roux et al.*, 1991] and one example at r = 8.8 R_E by *Lui et al.* [1992]. Both of these show a reduction in equatorial plasma pressure (plasma pressures from the *Roux et al.* [1991] example were evaluated by *Lyons* [1996]).

[5] In this paper, we use Geotail spacecraft measurements obtained near the midplane of the plasma sheet at r ~ 10–13 R_E to show that a reduction in equatorial pressure is a general feature of substorms and that this decrease is simultaneous with the well-known increase in energetic

[1]Department of Atmospheric Sciences, University of California, Los Angeles, Los Angeles, California, USA.
[2]Department of Earth and Planetary Sciences, Tokyo Institute of Technology, Tokyo, Japan.
[3]Institute of Space and Astronautical Science, Kanagawa, Japan.
[4]Department of Physics, University of Alberta, Edmonton, Alberta, Canada.

0148-0227/03/2003JA010177$09.00

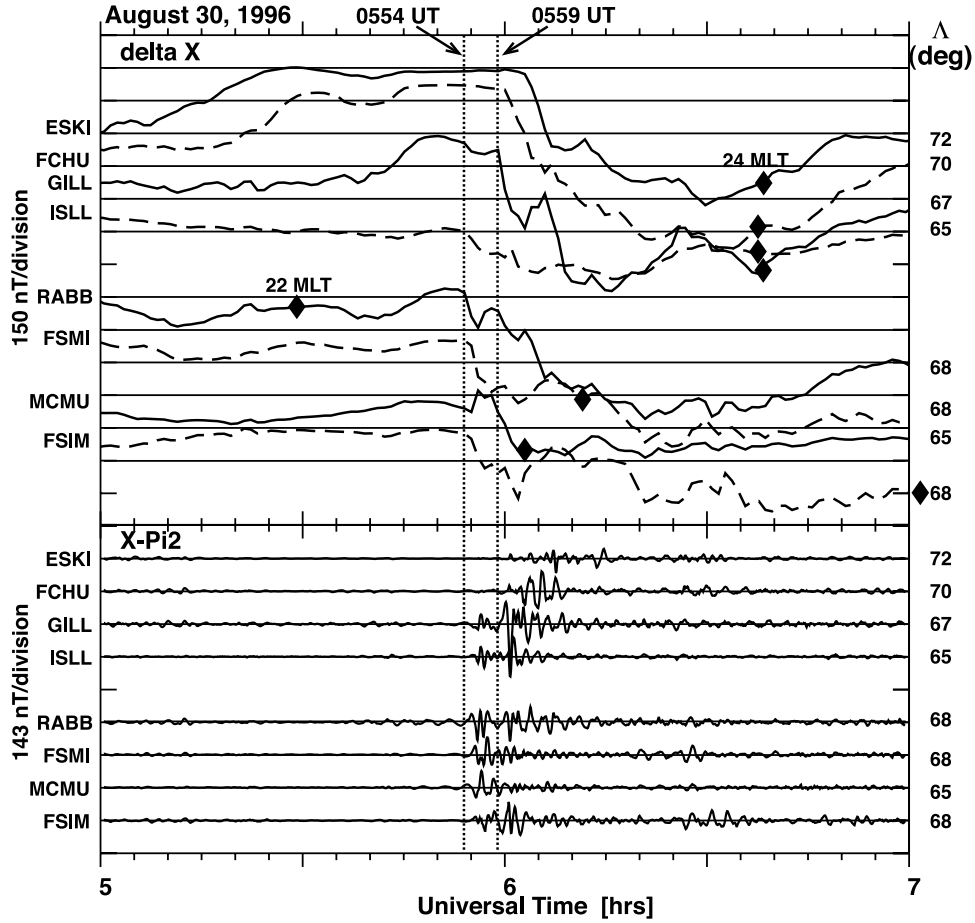

Figure 1. X-component and Pi2 observations from ground magnetometers of the Canadian Auroral Network for the OPEN Program Unified Study (CANOPUS) for 0500–0700 UT on 30 August 1996. Filled diamonds indicate the UT of 2400 MLT for the top four stations and of 2200 MLT for the bottom four stations. Vertical dotted lines indicate times of two expansion onsets.

particle fluxes and dipolarization of the magnetic field that occurs within the inner plasma sheet during the expansion phase. The decrease in pressure is found to be due to a decrease in particle fluxes at lower energies that gives a decrease in plasma density. We also show that when viewed as a function of the adiabatic energy invariant λ for isotropic plasma sheet particles, there is actually a reduction in particle fluxes at all λ despite the enhancements seen when energetic particle fluxes are viewed at fixed particle energy. These observations show that the expansion phase is associated with a significant reduction in flux tube content of particles within the current wedge, which implies there is a significant loss of plasma from current wedge flux tubes. In a companion paper [*Lyons et al.*, 2003], we investigate the cause of the reduction in flux tube content.

2. Observations

[6] Geotail has provided excellent coverage of plasma sheet substorm phenomena tailward of $r \approx 20\ R_E$, which is well beyond the region of substorm onset within the inner plasma sheet. Extensive analyses have also been performed of substorm observations from geosynchronous orbit, which is generally earthward of the region of current wedge formation at substorm onset [*Ohtani*, 1998]. However, the Geotail orbit in recent years has a perigee at $r \approx -10\ R_E$ and has thus given some coverage of the inner plasma sheet region where the substorm current wedge formation initiates. *Fairfield et al.* [1999] and *Nagai et al.* [2000] presented plasma sheet data at $x \approx -10$ to $-15\ R_E$ during the course of several substorms. Their emphasis was on the relationship between plasma flows and magnetic field dipolarizations and not on the evolution of particle distributions. Here, we examine particle distributions during six periods, which include 10 substorm onsets when Geotail was near the equatorial plane at $x \approx -10$ to $-13\ R_E$ and within a few R_E of $Y_{GSM} = 0$.

[7] Figure 1 shows X-component and Pi2 observations from ground magnetometers of the Canadian Auroral Network for the OPEN Program Unified Study (CANOPUS) for one of these periods, namely 0500–0700 UT on 30 August 1996. Data is shown from four stations located along the Ft. Churchill (FCHU) magnetic meridian and from four stations to the west of that meridian (See *Rostoker et al.* [1995] for full station names and exact station coordinates). The data show two closely spaced expansion phase onsets that were observed at ~2100 to ~2330 MLT, as was noted previously for this period by *Petrukovich et al.* [1999b]. The first was at 0554:30 UT and can be seen most clearly in the X-component at the three westernmost stations (RABB,

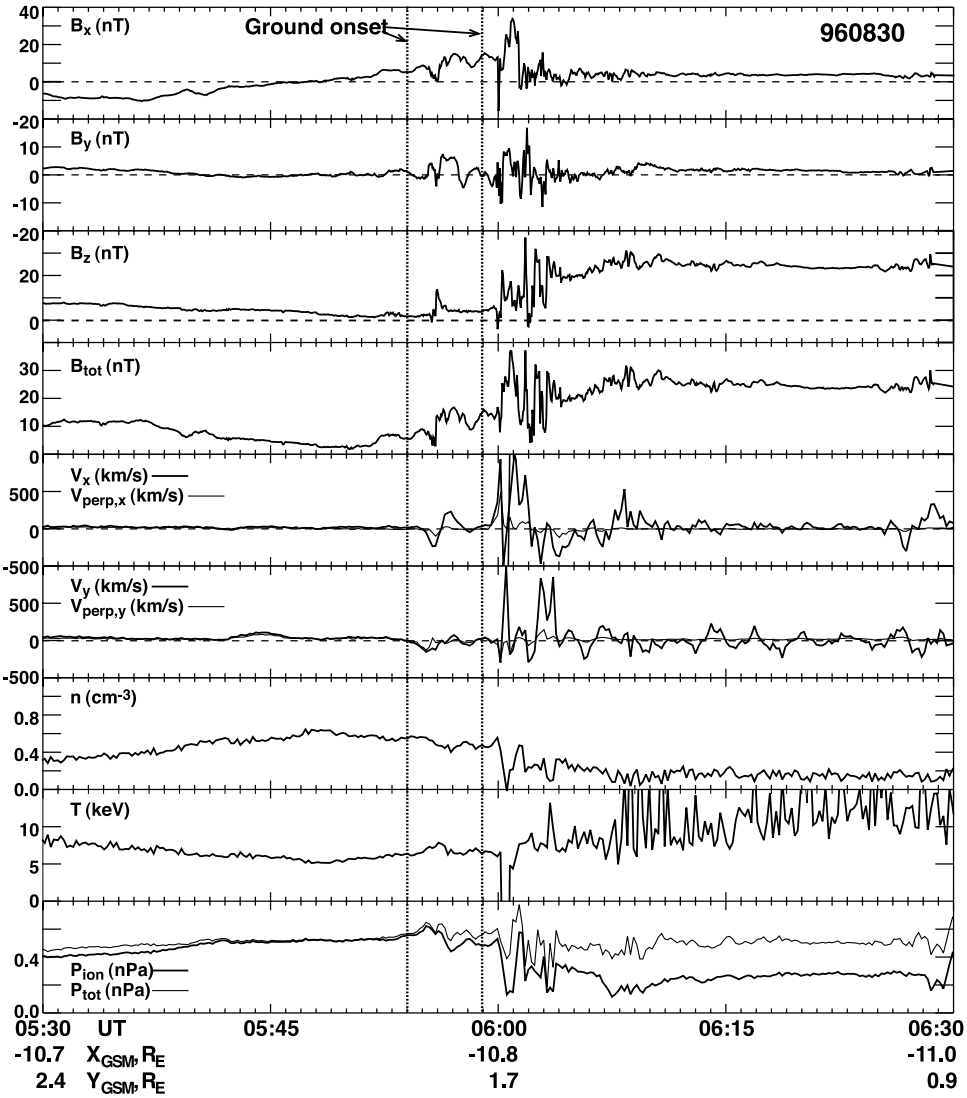

Figure 2. Magnetic fields and moments of LEP ions from 0530 to 0630 UT on 30 August 1996. Detector counts due to penetrating energetic electrons have been subtracted as described in Appendix A. $\mathbf{V}_{perp}$ is the component of ion velocity perpendicular to the measure magnetic field direction. P_{tot} is the sum of the ion and magnetic pressures.

FSMI, and FSIM) and as an onset of Pi2 pulsations seen at all longitudes. The second onset was at 0559 UT and can be seen most clearly in the X-component and as an enhancement of Pi2 pulsations along the Ft. Churchill meridian. It had a maximum X-component perturbation of ~600 nT at GILL and ~750 nT at FCHU, and thus was a moderate to large substorm. The above ground onset times are believed to be accurate to ~1 min.

[8] Magnetic fields [*Kokubun et al.*, 1994] and moments of 31 eV to 39 keV ions as measured by the Geotail low-energy plasma detector (LEP) [*Mukai et al.*, 1994] from 0530 to 0630 UT on 30 August 1996 are shown in Figure 2. Time resolution is 3 s for the magnetic field measurements and 12 s for the plasma measurements. In this example, and in several of our other examples, counts in the plasma detector due to penetrating energetic electrons were subtracted as described in Appendix A. This subtraction is necessary to obtain meaningful plasma moments and particle distributions when penetrating electron fluxes are significant, which occurs following several of the onsets considered here. The spacecraft was located at $X_{GSM} = -10.8\ R_E$ and $Y_{GSM} = 1.7\ R_E$ at the time of the onsets. The x-component of magnetic field B_x was below ~5 nT before 0551 UT and after 0603 UT, allowing good measurements to be obtained near the magnetic equator prior to and after the two onsets. Between 0551 and 0603 UT the spacecraft remained well within the central plasma sheet, except for an ~1 min period near 0600 UT when B_x and the ion pressure (P_{ion}) indicate a brief excursion to near the lobe. Prior to the onsets, P_{ion} gradually increased and B_z gradually decreased, as expected for a substorm growth phase.

[9] A small increase in B_z occurred ~1 min after the first ground onset, followed by a large increase in B_z ~1 min after the second onset. These B_z changes indicate that within the inner plasma sheet, a weak magnetic field dipolarization occurred following the first onset and a strong dipolarization occurred following the second onset.

These dipolarizations were accompanied, respectively, by a small decrease and a large decrease in P_{ion} and plasma density n. In this and our other examples it is not possible to determine precisely when these decreases initiated within the equatorial plane because of turbulence and changes in the spacecraft location relative to the equatorial plane (as indicated by B_x) that occurred near the time of onset. However, decreases relative to pre-onset values are clear in Figure 2 by 3 min after each onset. As discussed in section 1, a decrease in P_{ion} near the equator is expected to be associated with a reduction in cross-tail current within the current wedge but has not previously been shown to be a general feature of current wedge formation. An increase in ion temperature T occurred following the second onset in association with the large dipolarization of the magnetic field. (The enhanced noise of the density and temperature profiles after 0608 UT is a result of the enhanced counts from penetrating energetic electrons that occurred after this time and the subtraction of these counts.) The decrease in density associated with the onset is particularly important, since such a decrease is necessary for there to be a decrease in P_{ion} at the same time as T increases. Reductions in density together with increases in T have been previously observed within the plasma sheet in association with the substorm expansion phase [*Baumjohann et al.*, 1991; *Huang et al.*, 1992], though the observations used in these studies were generally obtained away from the equatorial plane.

[10] More details of the changes in the ion distribution in association with the two onsets can be seen in Figure 3. Figure 3 shows Geotail ion fluxes as a function of time from 0540 to 0620 UT for representative ion energies. Fluxes measured 16 times per spacecraft spin (spin axis perpendicular to the x,y-plane) have been averaged over 90° wide sectors centered on the $\pm X_{GSM}$ (sunward/tailward) and the $\pm Y_{GSM}$ (duskward/dawnward) directions. Line coding is used to indicate the different directions of particle motion as indicated in the figure, the heavy solid line indicating sunward directed ions. All fluxes that correspond to a count rate per spacecraft measurement of less than 1 have been plotted at the flux corresponding to the 1 count level. This gives a lower bound to fluxes that indicates background. Fluxes should only be regarded as being above background if they remain above the 1 count level for several consecutive measurements. Time series that appear as $\sim$1–2 point spikes above the 1 count level, as occurred for 325 eV electrons after 0554 UT, should thus be regarded as at background.

[11] Figure 3 shows that particle fluxes were generally the same in all directions, except for an enhancement in duskward fluxes relative to dawnward fluxes at higher energies before the onsets and structure just following each onset. The duskward enhancement prior to the onsets is the expected result of magnetic drift, which increases with increasing particle energy. The magnetic drift speed is inversely proportional to magnetic field magnitude and thus decreases significantly after the second onset. The structure just following the onsets occurs as the magnetic field dipolarizes and is an aspect of expansion phase turbulence. Such turbulence has been found to be a common expansion phase feature of the inner plasma sheet [*Lui et al.*, 1988, 1992].

[12] Notice from Figure 3 that both onsets were associated with a reduction in low-energy particle fluxes in all directions. This reduction can be seen at energies up to 2.6 keV after the first onset, and appears to have initiated $\sim$1–2 min prior to the ground onset (the slower variation prior to then was likely due to the spacecraft moving away from the midplane of the current sheet after crossing the midplane at $\sim$0548 UT, as indicated by B_x going through zero). The reduction is seen up to 13 keV after the second, and larger, onset. This reduction is seen starting $\sim$1–2 min after onset; however magnetic variations prevent a precise estimation of when the reduction actually initiated. The first onset brought the 325 eV fluxes to background levels and the 568 eV to very near background levels (the 163 eV fluxes reached background prior to this onset). Thus further flux reductions in these channels cannot be seen after the second onset. However, reductions are clear in the 906 eV to 13 keV channels. The second onset was also associated with a particle flux enhancement at the highest energy (39 keV) measured by the Geotail LEP detector. The weak dipolarization associated with the first onset did not lead to a high-energy flux increase detectable with the LEP detector. These increases, which are the typical substorm ''injection'' of energetic particles, are seen more readily at the higher energies covered by the Geotail energetic particle detector (EPIC) [*Williams et al.*, 1994]; however EPIC data was not available for the time period shown in Figures 1–3.

[13] Figure 4 shows X-component and Pi2 observations for 0700–0900 UT on 7 June 2000 from the same CANOPUS ground magnetometers as shown in Figure 1. Two onsets are clear in this figure, one at 0739 UT that was followed by a very small disturbance and one at 0753 UT that was followed by a moderate to large substorm. Geotail ($X_{GSM} \approx -12.6\ R_E$ and $Y_{GSM} \approx -0.7\ R_E$) magnetic fields and ion moments from 0730 to 0830 UT are shown in Figure 5. (LEP and EPIC observations are included in the ion moments, though inclusion of the EPIC observations does not significantly affect the moments.) B_x was near zero just before the first onset, during several periods between the two onsets, and after 0801 UT, allowing for measurements very near the equator before and after each onset. Like for the 30 August 1996 example, a weak dipolarization was observed following the first onset and a strong dipolarization occurred following the second onset, and these dipolarizations were accompanied, respectively, by a small decrease and a large decrease in P_{ion} and plasma density n. Considerable turbulence was observed for $\sim$15 min following the second onset, which is similar to the turbulence observed for a shorter period of time after the 0559 UT onset on 30 August 1996.

[14] Figure 6 shows Geotail LEP ion fluxes as a function of time from 0735 to 0815 UT on 7 June 2000 in the same format as Figure 3. Like for the 30 August 1996 onsets, a reduction in low energy ion fluxes was observed following both onsets on 7 June 2000. The decrease extended up to the 13 keV ion channel following the first onset and to the 23 keV channel following the second onset. (The turbulence following the second onset is also clear in the particle flux observations.) The first reduction appears to have initiated $\sim$1–2 min prior to the first ground onset and while, based on B_x, Geotail was very near the equator. The second reduction is seen starting $\sim$1 min after the second ground

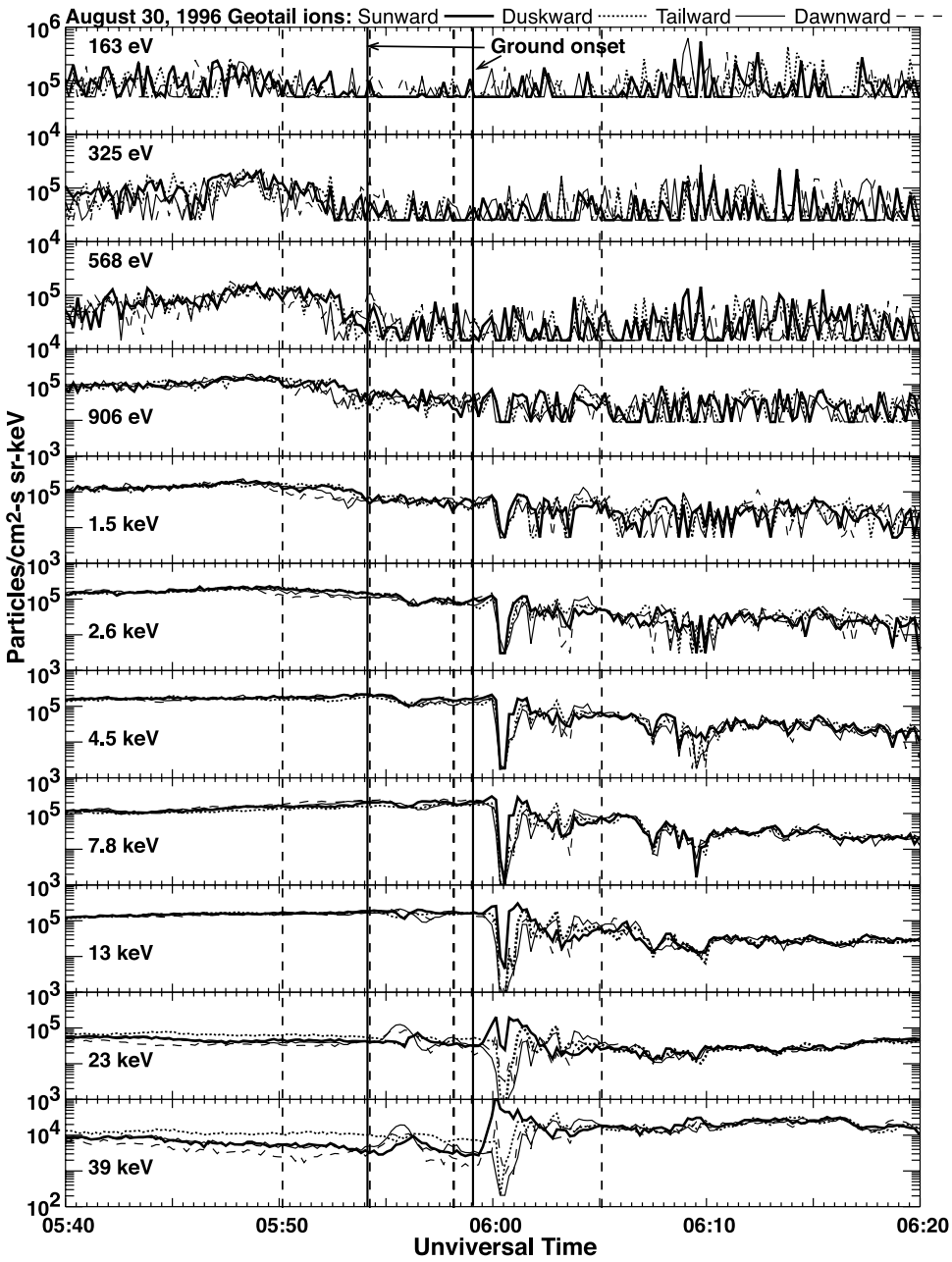

Figure 3. LEP ion fluxes as a function of time from 0540 to 0620 UT for representative energies. Fluxes measured 16 times per spacecraft spin (spin axis perpendicular to x, y-plane) have been averaged over 90° sectors centered on the $\pm X_{GSM}$ (sunward/tailward) and the $\pm Y_{GSM}$ (duskward/dawnward) going directions. Detector counts due to penetrating energetic electrons have been subtracted, and fluxes that correspond to a count rate per spacecraft measurement of less than 1 have been plotted at the flux corresponding to the 1 count level. Vertical solid lines indicate times of two expansion onsets. Vertical dashed lines indicate times of energy spectra shown in Figure 11.

onset; however, magnetic variations are quite significant during this period. Flux increases at higher energies can be seen in the LEP data at 23 and 39 keV following the first onset but are not clear in the LEP data following the second onset.

[15] For this period, however, energetic proton and electron observations from EPIC are available and are shown in Figure 7 in the same format as for the LEP data. The enhancement in energetic proton fluxes following both onsets are clear in the data, though the increase is difficult to see after the first onset in the 91 and 127 keV channels because preonset count rates for these channels were at background levels. The EPIC observations also show a significant increase in energetic electron fluxes following the second onset. (Energetic proton background counts affected the energetic electron measurements prior to the first onset (R. W. McEntire, private communication, 2003).) The increases were observed ~4 min after the second

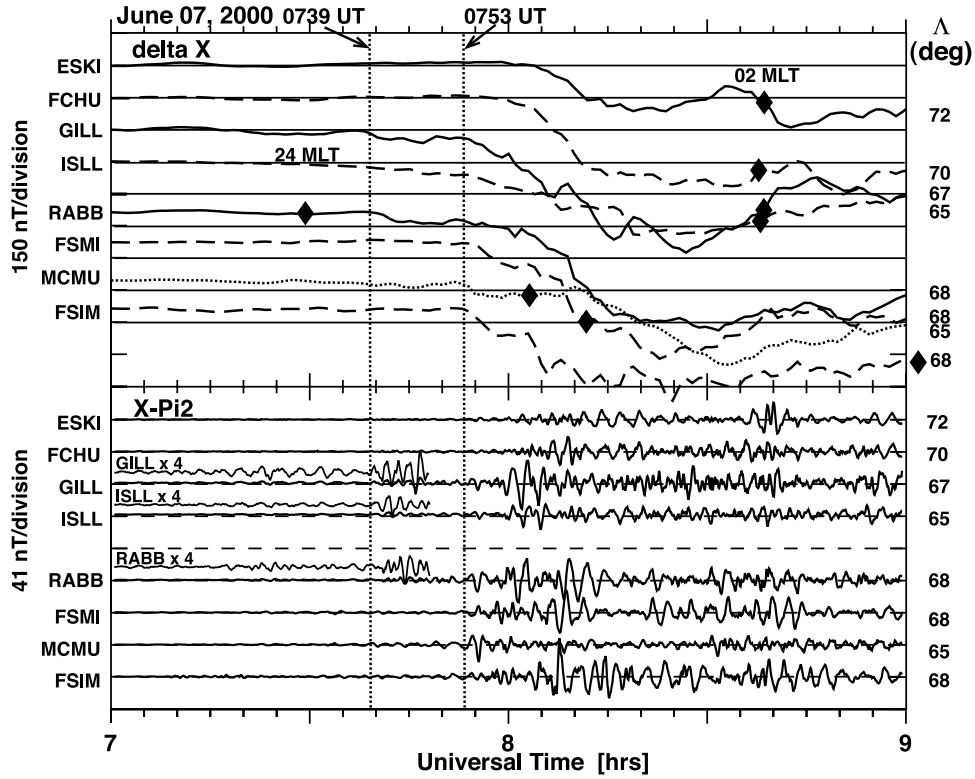

Figure 4. X-component and Pi2 observations from CANOPUS ground magnetometers for 0700–0900 UT on 7 June 2000. Filled diamonds indicate the UT of 0200 MLT for the top four stations and of 2400 MLT for the bottom four stations. Vertical dashed lines indicate the times of two expansion onsets.

ground onset, which may be related to Geotail being somewhat off of the equatorial plane during the first 4 min after the onset. These energetic proton and electron flux enhancements are the particle injections that are well known to occur within the inner plasma sheet in association with expansion phase magnetic field dipolarizations.

[16] Observations for a third example are shown in Figures 8–10 for a period on 14 August 1996 that included an onset of a very weak substorm at 0402 UT and of a small substorm at 0419 UT. Since these onsets occurred at earlier MLTs than for the previous examples, ground magnetometer data is shown for Poste-de-la-Beliene that was at ~2300 MLT at the time of the onsets and data from the westernmost CANOPUS stations are not shown. Also, the two onsets can be seen in auroral images from the POLAR spacecraft [see *Frank et al.*, 2001]. The Geotail observations for these two onsets show the same features as pointed out for the previous two examples, with the exception that the ion pressure showed a modest increase (by ~0.1 nPa), rather that a decrease following the first onset. Such an increase was not observed for any of the other 10 onsets included in the present study, and we do not have an explanation for why it happened in this case.

[17] The other four onsets were at 0655 UT on 8 June 1995, 0424 UT on 13 November 1996, and 1105 and 1116 UT on 4 September 1997. (Times for the 4 September 1997 onsets were obtained using Alaska chain as well as CANOPUS magnetometer data in order to include near-midnight MLTs.) These onsets all had the same ion flux, density, temperature and pressure changes noted for the six onsets discussed above. The only exception was for the 1105 UT onset on 4 September 1997. This was an onset of a weak substorm and a very small increase in ion pressure (by ~0.03 nP) and density (by 0.02 cm^{-3}) was observed. However, Geotail was slightly off the equator ($B_x \approx -5$ nT) before the onset and right at the equator ($B_x \approx 0$ nT) after the onset, so these small increases were likely related to the vertical structure of the plasma sheet. We have also examined the LEP and EPIC electron observations for all 10 onsets and have found that electron fluxes show the same features as do the ions, namely a decrease at lower energies and an increase at higher energies.

[18] Based on the observations for all 10 onsets, we conclude that the equatorial particle response of the substorm expansion phase within the nightside inner plasma sheet is generally characterized by: (1) a decrease in ion and electron fluxes at lower energies, (2) an increase in particle flux at higher energies, (3) a decrease in plasma density, (4) an increase in ion and electron temperatures, and (5) a decrease in plasma pressure. The only meaningful exception was the ion pressure increase during the weak first substorm on 14 August 1996.

3. Energy Spectra Changes and Adiabatic Compression

[19] Figure 11 shows ion energy spectra for times prior to (plus signs) and after (triangles) the ion flux and magnetic field changes associated with the six onsets in the examples

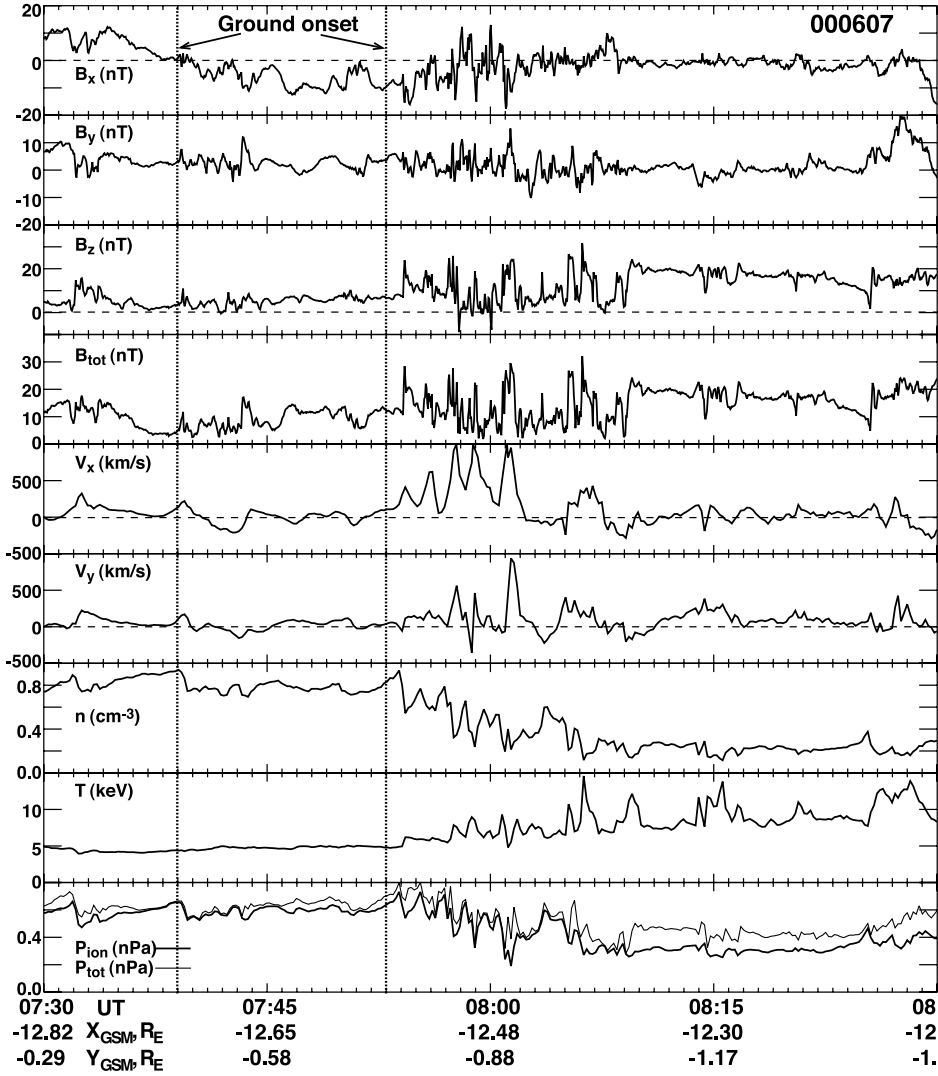

Figure 5. Magnetic fields and ion moments from 0730 to 0830 UT on 7 June 2000. LEP and EPIC observations are included in the ion moments. $\mathbf{V}_{perp}$ was not available from DARTS for this interval.

discussed above. All measured fluxes values above background are shown from the LEP detector and, for 7 June 2000, from EPIC. Times were selected to be when the spacecraft was as close to the center of the plasma sheet as possible (as small as possible $|B_x|$) and to also be either as close in time as possible before the onset or just after the turbulence that follows the onset. Vertical dashed lines in Figures 3, 6, 7, and 10 identify the selected times.

[20] The energy spectra in Figure 11 clearly show the drop in fluxes at lower energies and the enhancement in fluxes at the higher energies that we have found to be associated with the substorm expansion phase within the inner plasma sheet. The transition between decreased and increased fluxes occurs at an energy that, based on all 10 onsets, ranges from ~3.5 keV (the 0554 UT onset on 30 August 1996) to ~35 keV (the 0419 UT onset on 14 August 1996).

[21] The above comparisons are of particle fluxes j(K) measured as a function of ion kinetic energy. However, the B_z increase associated with substorm onset implies a significant decrease in flux tube volume and an accompanying significant adiabatic change in particle energies. Adiabatic motion of an isotropic particle distribution within a flux tube gives conservation of the adiabatic energy invariant $\lambda = K\mathcal{V}^{2/3}$, where K is particle kinetic energy [e.g., *Wolf*, 1983; *Heinemann*, 1999]. Dipolarization of the magnetic field within the current wedge causes a decrease in $\mathcal{V}$ and would thus cause an increase in K. Thus a more meaningful comparison of the energy spectra obtain before and after the onsets is of phase space density f as a function of the energy invariant $\lambda = K\mathcal{V}^{2/3}$. This is equivalent to comparing the energy spectra measured after each onset $j_f(K)$ to $j_{ad}(K_{ad}) = (K_{ad}/K_i)j_i(K_i)$, since $f(K) \propto j(K)/K$ and conservation of λ causes particles of an initial energy K_i to increase their energy to $K_{ad} = K_i[\mathcal{V}_i/\mathcal{V}_f]^{2/3}$. Here j_i is the flux measured before each onset, and $\mathcal{V}_i$ and $\mathcal{V}_f$ are flux tube volume before and after onset, respectively. The spectra $j_{ad}(K_{ad})$ can be viewed as the spectra that would result if all particles contributing to $j_i(K_i)$ were adiabatically energized by the decrease in volume from $\mathcal{V}_i$ to $\mathcal{V}_f$ and there were no sources or losses of particles from a flux tube.

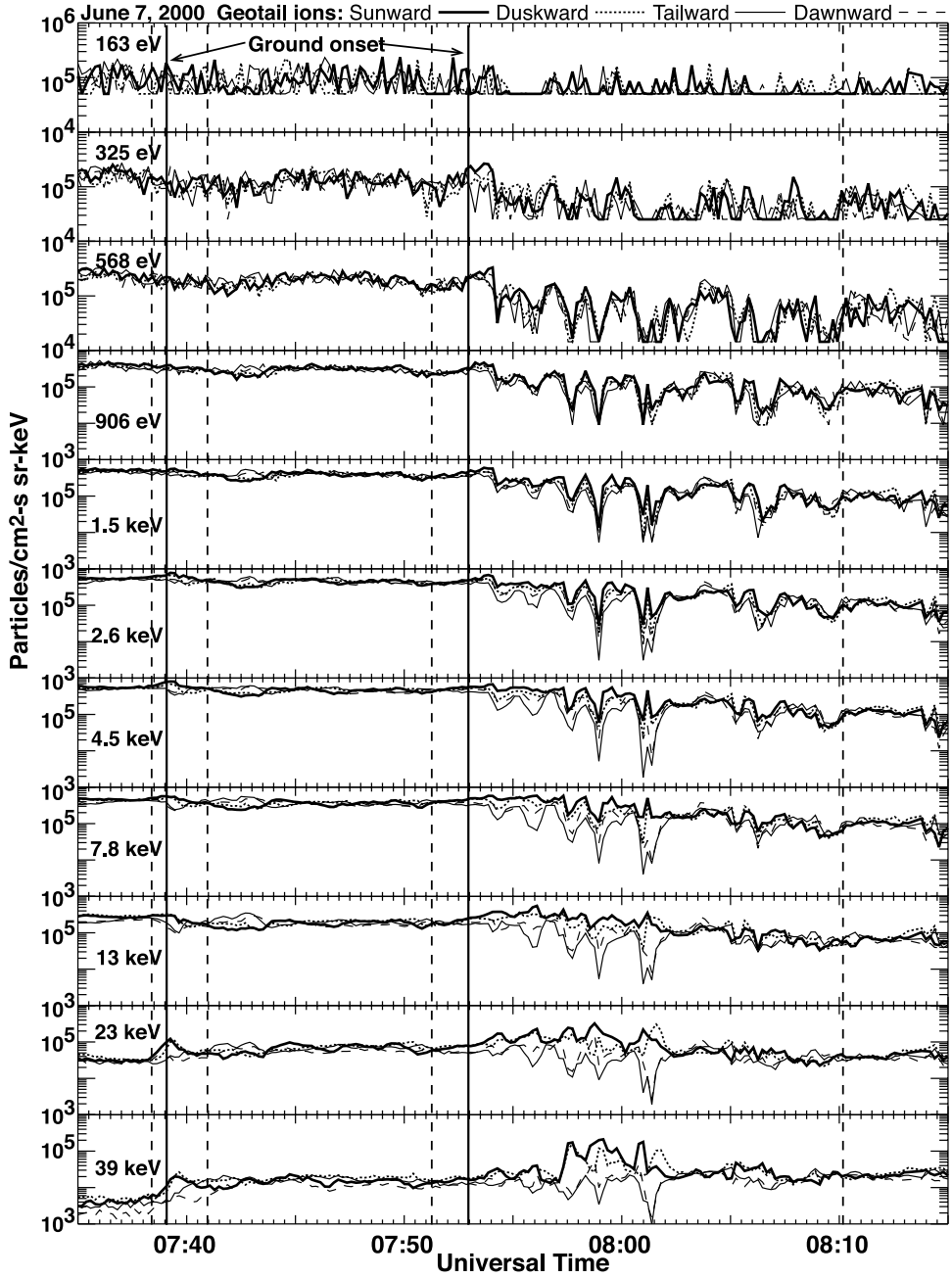

Figure 6. LEP ion fluxes as a function of time from 0735 to 0815 UT on 7 June 2000 in the same format as Figure 3.

[22] While it is not possible to measure $\mathcal{V}_i$ and $\mathcal{V}_f$, we have made simple estimates for the ratios of these volumes using the measured values of B_z. To do this, we first evaluated the equatorial B_z and flux tube volume using the Tsyganenko 96 (T96) magnetic field model [*Tsyganenko*, 1995, 1996] for different geomagnetic activity levels and a large number of locations within the region $-9\ R_E > X_{GSM} > -20\ R_E$ and $|YGSM| < 5$ RE (the values of the T96 input parameters we used were: solar wind dynamic pressure = i nPa, Dst = $-6 \times$ i nT, IMF $B_y = 0$, and IMF $B_z = -1 \times$ i nT, where i is a constant that varies from 1 to 9). We found that the variation of the flux tube volume with magnetic field strength falls approximately between the curves $\mathcal{V} \propto B_z^{-3/2}$ and $\mathcal{V} \propto B_z^{-1}$. We thus used the values of B_z measured at the times of each energy spectra, which are given in Figure 11, and evaluated $j_{ad}(K)$ under the assumption that $KB_z^{-2/3}$ is conserved and under the assumption that KB_z^{-1} is conserved. (Conservation of KB_z^{-1} would also apply to equatorially mirroring particles if the first adiabatic moment were conserved.)

[23] The calculated spectra $j_{ad}(K_{ad})$ under the two assumptions are shown in Figure 11. Since comparing $j_{ad}(K_{ad})$ to $j_f(K)$ is equivalent to comparing $f_f(\lambda)$ to $f_i(\lambda)$, Figure 11 shows that the substorm expansion is associated with a reduction in the number of particles at essentially all measured λ within the inner plasma sheet. Conservation of

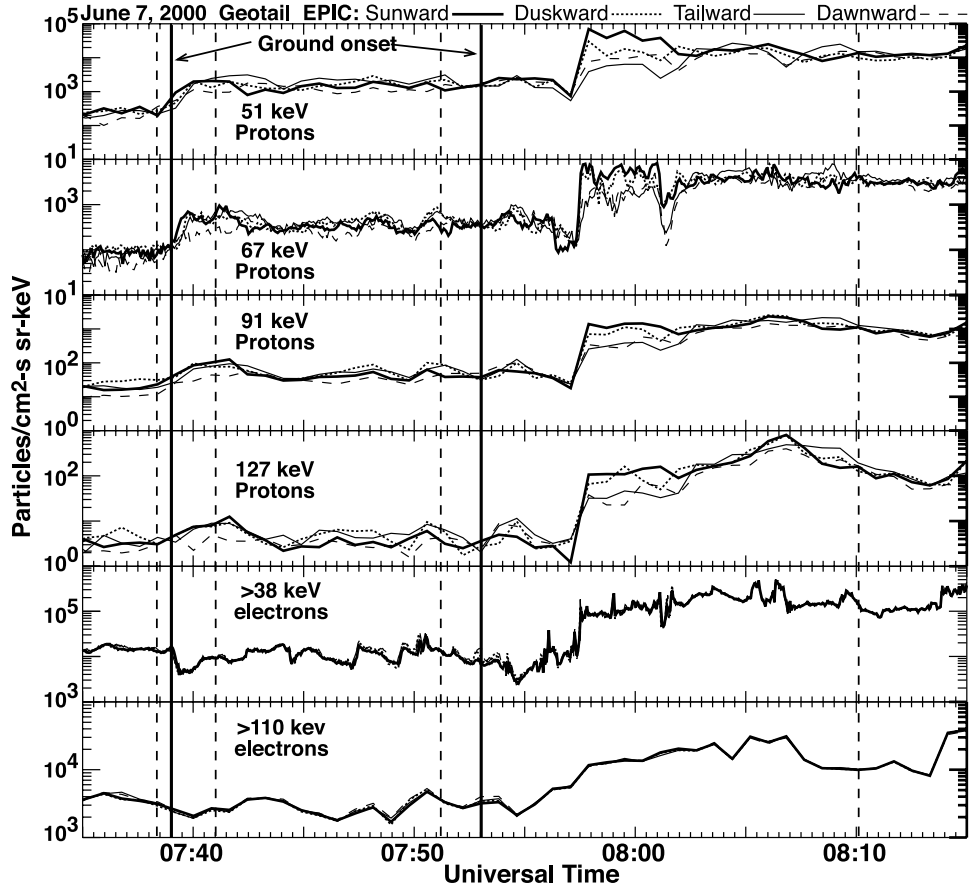

Figure 7. EPIC ion and electron fluxes as a function of time from 0735 to 0815 UT on 7 June 2000 in the same format as Figure 3.

f(λ) for all λ would give conservation of flux tube content n$\mathcal{V}$ and thus would lead to an increase in plasma density n when $\mathcal{V}$ decreases. However, the reductions in f(λ) are sufficiently large that there is a reduction in plasma pressure and density after the decrease in $\mathcal{V}$. This implies that there is a very significant reduction in the total flux tube content within the inner plasma sheet associated with the substorm expansion phase, and that reduction occurs for all λ.

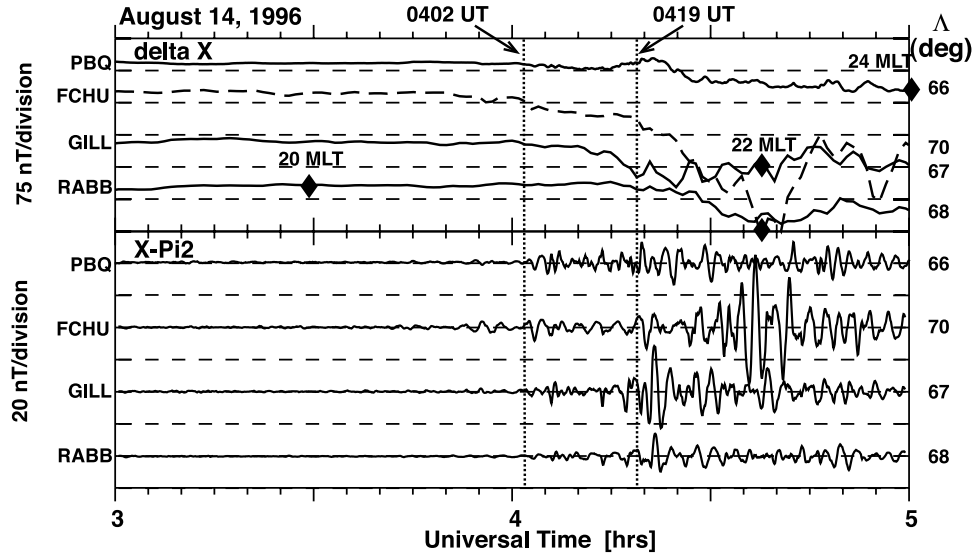

Figure 8. X-component and Pi2 observations ground magnetometers for 0300–0500 UT on 14 August 1996. Data is shown for Poste-de-la-Beliene (PBQ) that was at ~2300 MLT at the time of the onsets and data from the westernmost CANOPUS stations is not shown. From top to bottom, filled diamonds indicate the UT of 2400, 2200, 2200, and 2000 MLT. Vertical dashed lines indicate the times of two expansion onsets.

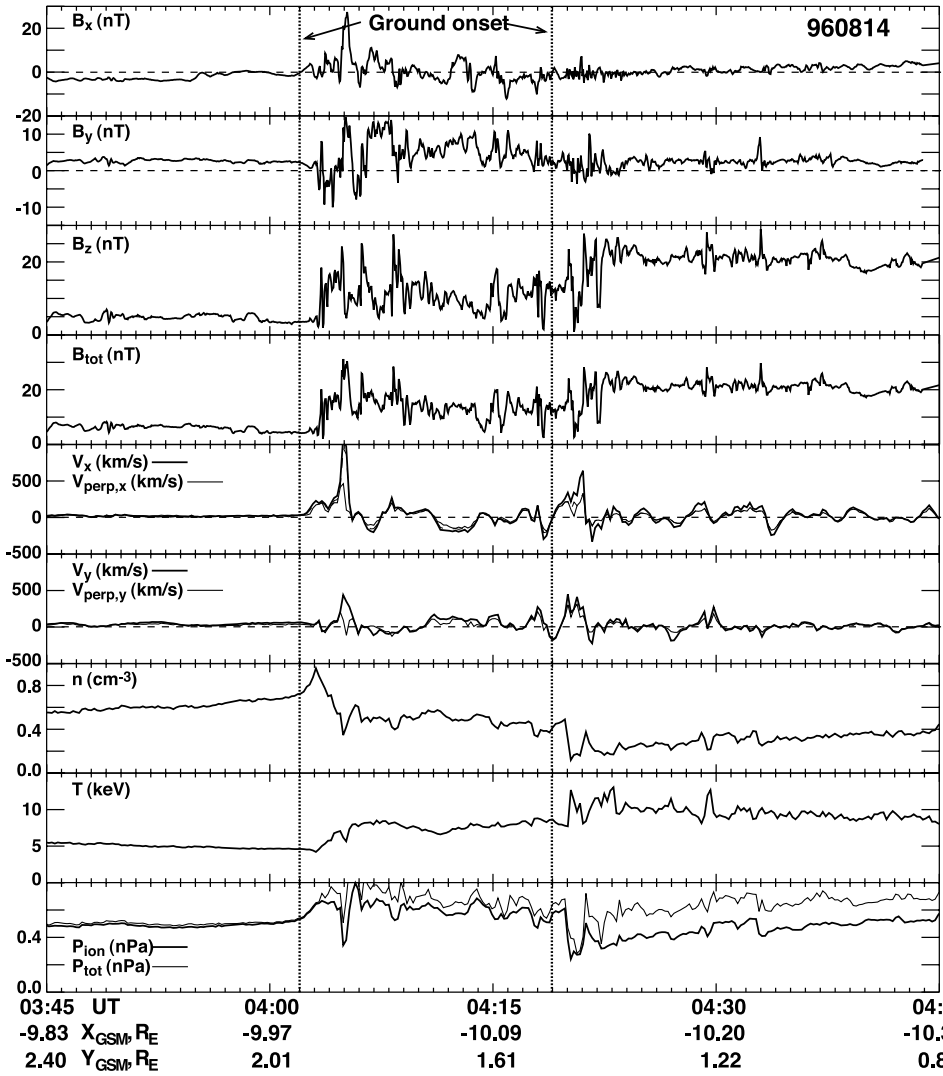

Figure 9. Magnetic fields and moments of LEP ions from 0350 to 0430 UT on 14 August 1996.

Understanding the substorm expansion phase thus requires understanding the significant reduction of plasma content of flux tubes within the inner plasma sheet.

4. Summary and Conclusions

[24] We have presented Geotail spacecraft measurements obtained near the center of the plasma sheet at $r \sim 10-13\ R_E$ and found that a reduction in equatorial proton pressure is a general feature of substorms. While temperature increases in association with the dipolarization of the magnetic field within the current wedge, the plasma density decreases as the current wedge forms. The decrease in density is large enough that it leads to a decrease in pressure despite the concurrent increase in temperature. Combining the decrease in density with the decrease in flux tube volume that also occurs as the magnetic field dipolarizes shows that there is a large reduction in flux tube ion content within the current wedge.

[25] We have found that the decrease in ion pressure, density, and flux tube content within the current wedge occurs simultaneously with an increase in energetic particle fluxes. A decrease in ion fluxes at lower energies gives the observed decrease in pressure and density, and a transition from decreasing to increasing ion fluxes occurs at an energy between ~3.5 and ~35 keV. While enhancements are seen when energetic particle fluxes are viewed at fixed particle energy, we find that the ion distribution function decreases at all invariant energies λ. Thus there is a significant loss of ions from flux tubes at all λ during the substorm expansion phase. We have also found that electron fluxes within the current wedge show the same general features as do the ion fluxes, namely a decrease at lower energies and an increase at higher energies.

[26] The observations show evidence that low-energy ion fluxes begin to decrease a few min prior to ground onset, whereas the plasma moments do not show a consistent change prior to onset. It would be desirable to reliably determine when these changes initiate within the equatorial inner plasma sheet relative to the time of ground onset. However, motion of the spacecraft relative to the equatorial plane and magnetic turbulence associate with the onsets preclude us from making such a determination with the present observations.

[27] In a companion paper [*Lyons et al.*, 2003], we investigate the cause of the reduction in flux tube content.

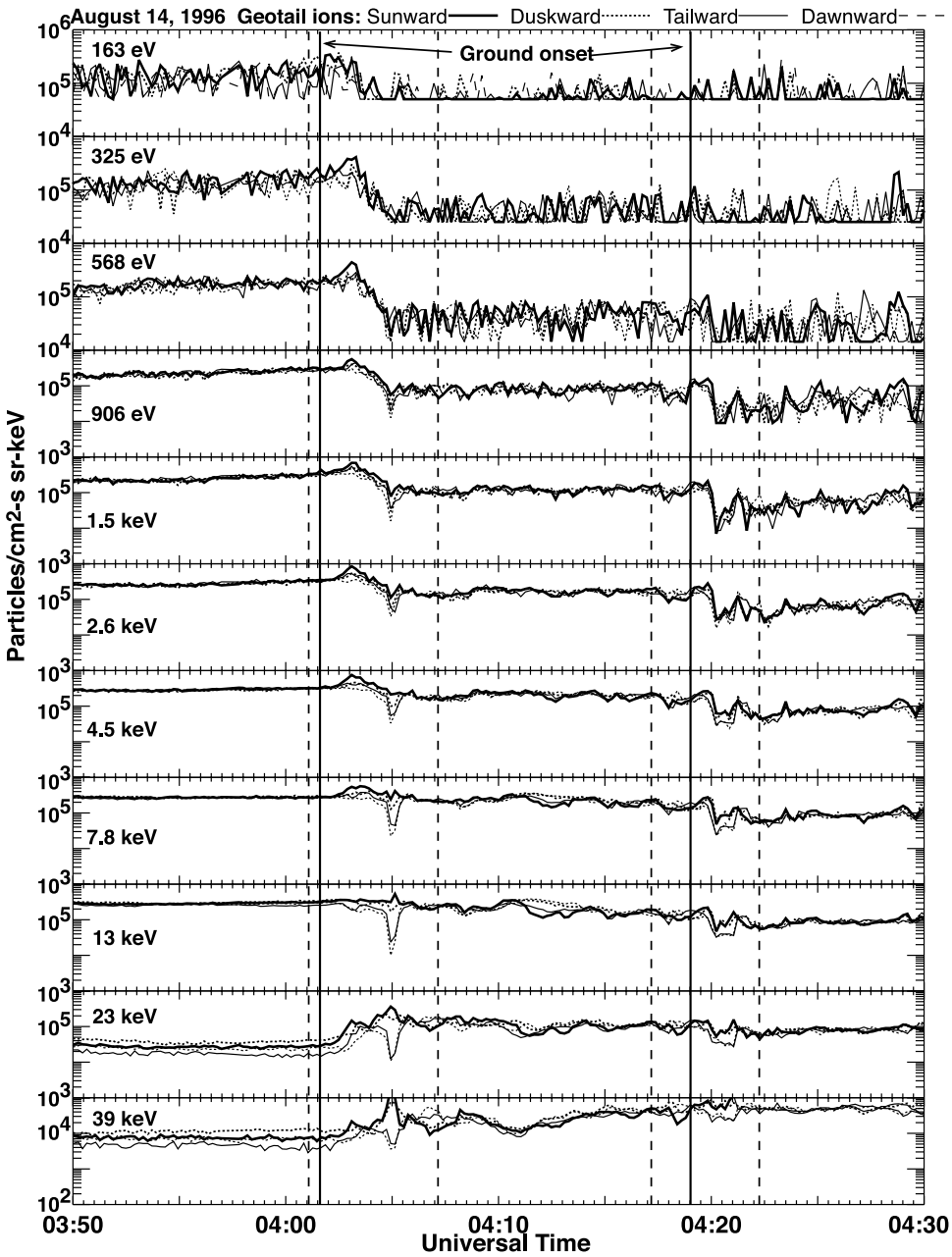

Figure 10. LEP ion fluxes as a function of time from 0350 to 0430 UT on 14 August 1996 in the same format as Figure 3.

We apply the continuity equation for plasma sheet particles derived by *Heinemann* [1999] and find that a reduction in the strength of convection following a period of enhanced convection should cause a divergence of plasma sheet particles that is driven by magnetic drift. This divergence is found to give a reduction in flux tube content within the premidnight to midnight region of the Harang discontinuity and to offer a plausible explanation for current wedge formation and thus the initiation of the substorm expansion phase.

Appendix A

[28] *Fairfield et al.* [1998] and *Nagai et al.* [2000] noted that within the inner plasma sheet, particle measurements by the Geotail LEP detector can be affected by penetrating energetic electrons. Penetrating electrons are identifiable as isotropic background count rates that are independent of particle energy. The effects of these background counts are most important in the lowest energy channels, where, as can be seen from Figure 11, particle fluxes are nearest the 1 count per measurement flux level. When present, it is necessary to subtract the counts due to penetrating energetic electrons in order to obtain meaningful variations with time of low-energy particle fluxes and meaningful plasma moments. Penetrating electrons effected the LEP measurements during four of the six intervals considered in this paper (14 August 1996, 30 August 1996, 11 September 1997, and 6 June 2000). Below we describe how we identified counts due

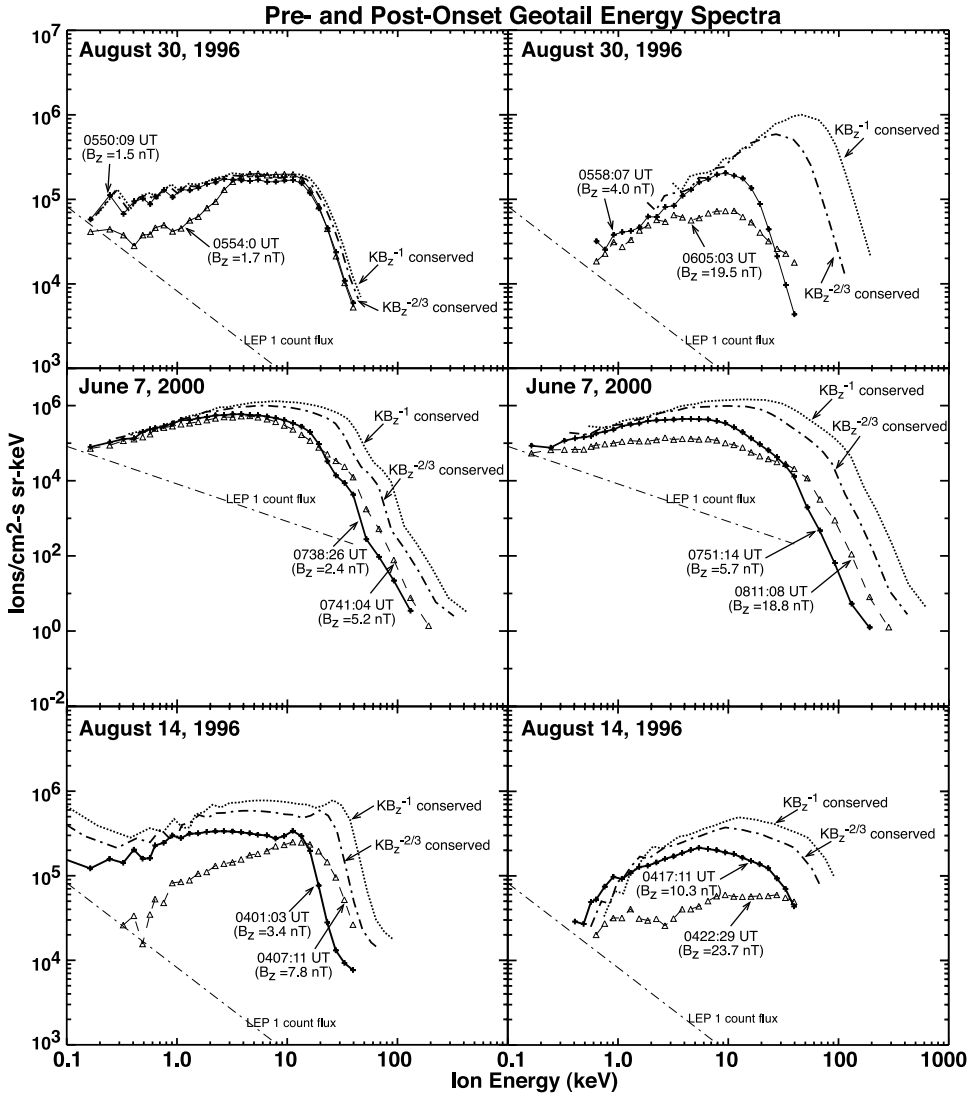

Figure 11. Ion fluxes versus energy for times prior to (plus signs) and after (triangles) the flux and magnetic field changes of the six onsets in Figures 1–10. All measured fluxes values above background are shown from the LEP detector and, when available, from EPIC. Vertical dashed lines in Figures 3, 6, and 9 identify the selected times. Also shown are fluxes versus energy that would result from adiabatic energization of the prior to energy spectra, with no sources or losses of particles from a flux tube, assuming $\mathcal{V} \propto B_z^{-3/2}$ (KB_z^{-1} conserved) and $\mathcal{V} \propto B_z^{-1}$ ($KB_z^{-1/3}$ conserved).

to penetrating electrons and how their effects were subtracted.

[29] The upper portion of Figure 12 shows the LEP average count rates per spacecraft measurement for the 30 August 1996 period for selected energy channels and for each of the four 90° wide angular sectors shown in Figure 3. Also shown by the thick dashed line in each panel is the count rate for the lowest energy channel (31 eV) averaged over all look directions. At the lower energies, count rates for all look directions can be seen to be equal, to within counting statistics, to the average count rate of the 31 eV channel. This equality identifies these counts as being due to penetrating electrons. Penetrating electrons can be seen to have given ~10 counts per spacecraft measurement prior to 0600 UT. A large increase in the penetrating electron counts occurred after the 0559 UT substorm onset, which presumably resulted from a substorm-associated increase in energetic electron fluxes. Count rates that exceedthe penetrating electron background for a particular energy channel represent actual measurements of particles within the energy range of that channel. In Figure 12, a transition to count rates above background levels can be seen at energies ≥325 eV at ~0545–0550 UT and at energies ≥1.2 keV after 0600 UT.

[30] To correct for the penetrating electrons, we have subtracted the average count rate in the 31 eV channel, averaged over all look directions, from the average count rate in each 90° wide angular sector for all energy channels. This subtraction gives the count rates shown for four representative energies in the lower portion of Figure 12. This leads to statistical variations of the count rates that increase with the penetrating electron count rate. However,

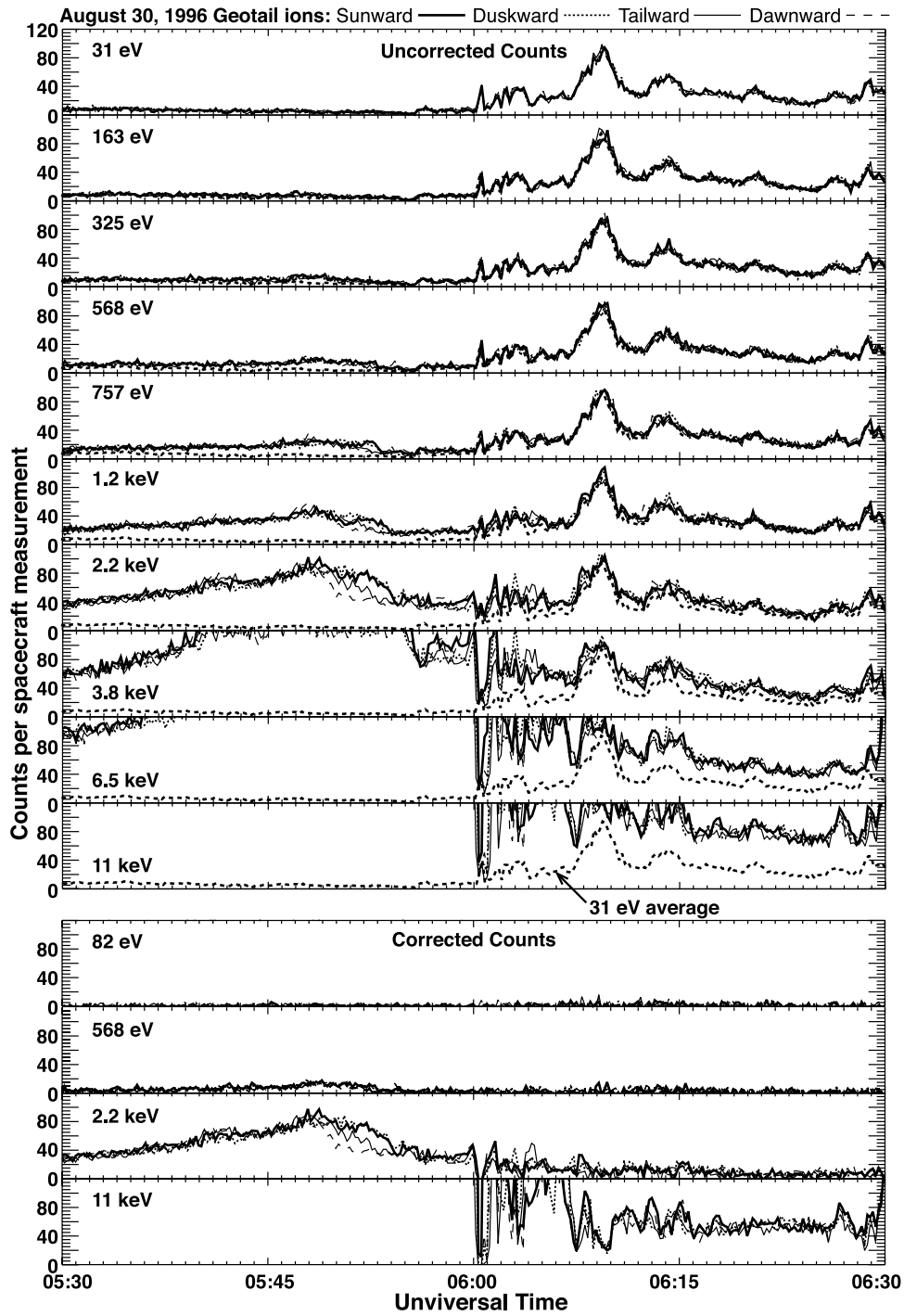

Figure 12. LEP measurements for the 30 August 1996 period for selected energy channels and for each of the four 90° wide angular sectors shown in Figure 3. Upper portion: Average count rates per spacecraft measurement. Thick dashed line in each panel gives the count rate for the lowest energy channel (31 eV) averaged over all look directions. Lower portion: Average count rates after subtraction of the 31 eV channel count rates averaged over all look directions.

this increase does not present a significant problem and the increases in count rates at higher energies to levels above background can clearly be seen.

[31] As a check on our identification of the isotropic background counts as being due to penetrating energetic electrons, we show in Figure 13 comparisons between the 31 eV ion fluxes obtained without correction and fluxes from the highest energy EPIC electron channel (>110 keV). We do not know the precise minimum electron energy needed to penetrate the LEP detector; however, the comparisons in Figure 13 indicate that the >110 keV fluxes give a good measure of the fluxes of penetrating electrons. Comparisons are shown for 1 hour periods for each of the four of our event periods for which EPIC data is available.

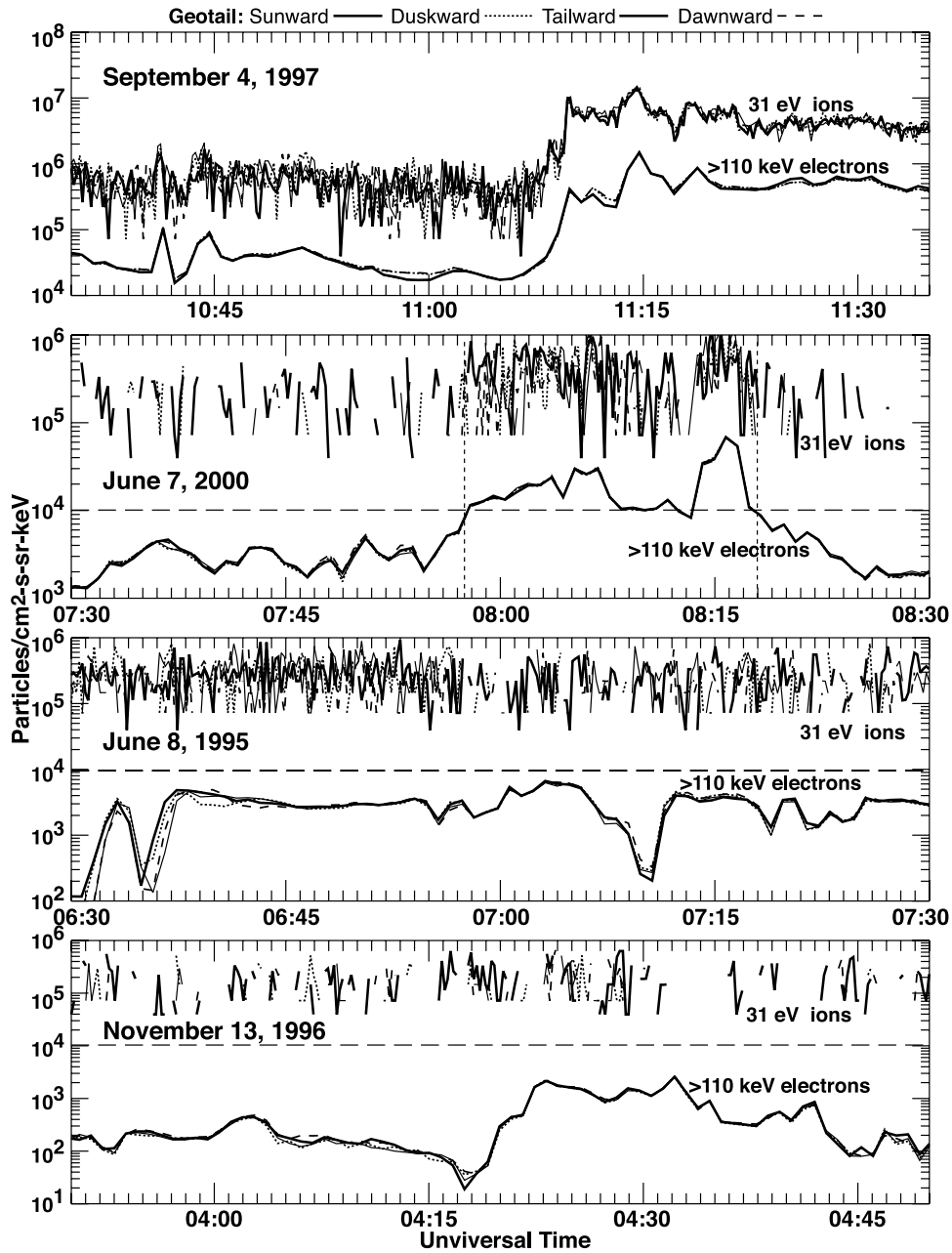

Figure 13. Comparisons between the 31 eV ion fluxes without correction for penetrating electron counts and fluxes from the highest energy EPIC electron channel (>110 keV). Horizontal dashed line at >110 keV electron flux of 10^4 electrons/cm^2-sr-keV identifies threshold above which counts from penetrating electrons are significant. Vertical short-dashed lines in the 7 June 2000 panel identify times used for determining flux threshold.

[32] The >110 keV electron fluxes were largest for the 4 September 1997 period. For this period, the 32 eV LEP ion fluxes almost exactly track the >110 keV electron fluxes. This is strong evidence that the 32 eV count rates where dominated by penetrating energetic electrons and that the >110 keV electron measurements gives a good measure of the flux of penetrating electrons. The observations on 7 June 2000 allow us to set a flux threshold of $\sim 10^4$ electrons/cm^2-sr-keV for >110 keV electrons, above which counts from penetrating electrons are significant. It can be seen that count rates in the 32 eV ion channel were at or close to zero when >110 keV electron fluxes were below 10^4 electrons/cm^2-sr-keV. The 32 eV count rates only became significantly nonzero between 0758 and 0818 UT, when the >110 keV electron fluxes exceeded 10^4 electrons/cm^2-sr-keV. Also, considering the low count rates, the 32 eV ion fluxes track the >110 keV electron fluxes quite well during that time interval. Consistent with the above threshold, the >110 keV electron fluxes remained below 10^4 electrons/cm^2-str-keV during the 13 November 1996 period and 32 eV ion count rates remained near zero. The >110 keV electron fluxes also

remained below 10^4 electrons/cm^2-str-keV during the 8 June 1995 period. The 32 eV ion count rates remained low during this period and do not appear to track the >110 keV electron fluxes, suggesting that low count rates of 32 eV ions may have been measured. There may be some effects from penetrating electrons, however, since the >110 keV electron fluxes were only slightly below 10^4 electrons/cm^2-sr-keV for much of the period.

[33] **Acknowledgments.** This research was supported at UCLA in part by NSF grants OPP-0136139 and ATM-0207298. Research support for J. C. Samson was in part by the Natural Sciences and Engineering Research Council of Canada. CANOPUS data have been obtained with support of the Canadian Space Agency. We acknowledge the efforts of D. Wallis, who is responsible for the operations of the CANOPUS magnetometers. The magnetometer at Poste de la Baleine is operated by the National Geomagnetism Program of the Canadian Geological Survey. Alaska chain magnetometer data was provided by John Olson of the Geophysical Institute of the University of Alaska. We also thank Richard McEntire and Jon Vandegriff of the Applied Physics Laboratory for providing the Geotail EPIC data used in this study. GEOTAIL magnetic fields were provided by S. Kokubun, through DARTS at the Institute of Space and Astronautical Science (ISAS) in Japan. Finally, we thank G. Erickson and A. Nishida for carefully reading a draft of this paper.

[34] Arthur Richmond thanks Atsuhiro Nishida and another reviewer for their assistance in evaluating this paper.

References

Baumjohann, W. J., G. Paschmann, T. Nagai, and H. Lühr, Superposed epoch analysis of the substorm plasma sheet, *J. Geophys. Res.*, *96*, 11,605, 1991.

Caan, M. N., R. L. McPherron, and C. T. Russell, Substorm and interplanetary magnetic field effects on the geomagnetic tail lobes, *J. Geophys. Res.*, *80*, 191, 1975.

Fairfield, D. H., et al., Geotail observations of substorm onset in the inner magnetotail, *J. Geophys. Res.*, *103*, 103, 1998.

Fairfield, D. H., et al., Earthward flow bursts in the inner magnetosphere and their relation to auroral brightenings, AKR intensifications, geosynchronous particle injections and magnetic activity, *J. Geophys. Res.*, *104*, 355, 1999.

Frank, L. A., W. R. Paterson, and J. B. Sigwarth, Observations of plasma sheet dynamics earthward of the onset region with the Geotail spacecraft, *J. Geophys. Res.*, *106*, 18,823, 2001.

Heinemann, M., Role of collisionless heat flux in magnetospheric convection, *J. Geophys. Res.*, *104*, 28,397, 1999.

Huang, C. Y., L. A. Frank, G. Rostoker, J. Fennell, and D. G. Mitchell, Nonadiabatic heating of the central plasma sheet at substorm onset, *J. Geophys. Res.*, *97*, 1481, 1992.

Jacquey, C., J. A. Sauvaud, and J. Dandouras, Location and propagation of the magnetotail substorm expansion: Analysis and simulation of an ISEE multi-onset event, *Geophys. Res. Lett.*, *18*, 389, 1991.

Jacquey, C., J. A. Sauvaud, and J. Dandouras, Tailward propagating tail current disruption and dynamics of the near-Earth tail: A multi-point measurement analysis, *Geophys. Res. Lett.*, *20*, 983, 1993.

Kokubun, S., T. Yamamoto, M. H. Acuña, K. Hayashi, K. Shiokawa, and H. Kawano, The Geotail magnetic field experiment, *J. Geomagn. Geoelectr.*, *46*, 7, 1994.

Lui, A. T. Y., et al., A case study of magnetotail current disruption and diversion, *Geophys. Res. Lett.*, *15*, 721, 1988.

Lui, A. T. Y., et al., Current disruptions in the near-Earth neutral sheet region, *J. Geophys. Res.*, *97*, 1461, 1992.

Lyons, L. R., Theory for substorms triggered by sudden reductions in convection, in *Third International Conference on Substorms (ICS-3)*, p. 126, Eur. Space Agency, Noordwijk, Netherlands, 1996.

Lyons, L. R., C.-P. Wang, and T. Nagai, Substorm onset by plasma sheet divergence, *J. Geophys. Res.*, *108*, doi:10.1029/2003JA010178, in press, 2003.

McPherron, R. L., C. T. Russell, and M. P. Aubry, Satellite studies of magnetospheric substorms on August 15, 1968: 9. Phenomenological model of substorms, *J. Geophys. Res.*, *78*, 3131, 1973.

Miyashita, Y., S. Machida, S. T. Mukai, Y. Saito, K. Tsuruda, H. Hayakawa, and P. R. Sutcliffe, A statistical study of variations in the near and mid-distant magnetotail associated with substorm onsets: GEOTAIL observations, *J. Geophys. Res.*, *105*, 15,913, 2000.

Moore, T. E., R. L. Arnoldy, J. Feynman, and D. A. Hardy, Propagating substorm injection fronts, *J. Geophys. Res.*, *86*, 6713, 1981.

Mukai, T., S. Machida, Y. Saito, M. Hirahara, T. Terasawa, N. Kaya, T. Obara, M. Ejiri, and A. Nishida, The low-energy particle (LEP) experiment onboard the Geotail satellite, *J. Geomagn. Geoelectr.*, *46*, 669, 1994.

Nagai, T., H. Singer, T. Mukai, T. Yamamoto, and S. Kokubun, Development of substorms in the near-Earth tail, *Adv. Space Res.*, *25*, 1651, 2000.

Ohtani, S., Earthward expansion of tail current disruption: Dual-satellite study, *J. Geophys. Res.*, *103*, 6815, 1998.

Ohtani, S., S. Kokubun, and C. T. Russell, Radial expansion of the tail current disruption during substorms: A new approach to the substorm onset region, *J. Geophys. Res.*, *97*, 3129, 1992.

Petrukovich, A. A., T. Mukai, S. Kokubun, S. A. Romanov, Y. Saito, T. Yamamoto, and L. M. Zelenyi, Substorm associated pressure variations in the magnetotail plasma sheet and lobes, *J. Geophys. Res.*, *104*, 4501, 1999a.

Petrukovich, A. A., J. Wanliss, T. Mukai, S. Kokubun, and T. Yamamoto, Small amplitude bipolar flows in the near-Earth tail, *Geophys. Res. Lett.*, *26*, 2909, 1999b.

Rostoker, G., et al., CANOPUS-A ground-based instrument array for remote sensing the high latitude ionosphere during the ISTP/GGS program, *Space Sci. Rev.*, *71*, 743, 1995.

Roux, A., et al., Plasma sheet instability related to the westward traveling surge, *J. Geophys. Res.*, *95*, 17,697, 1991.

Samson, J. C., L. R. Lyons, B. Xu, F. Creutzberg, and P. Newell, Proton aurora and substorm intensifications, *Geophys. Res. Lett.*, *19*, 2167, 1992.

Tsyganenko, N. A., Modeling the Earth's magnetospheric magnetic field confined within a realistic magnetopause, *J. Geophys. Res.*, *100*, 5599, 1995.

Tsyganenko, N. A., Effects of the solar wind conditions on the global magnetospheric configuration as deduced from data-based field models, in *Proceedings of the ICS-3 Conference on Substorms*, *ESA SP-389*, pp. 181–185, Eur. Space Agency, Noordwijk, Netherlands, 1996.

Williams, D. J., R. W. McEntire, C. Schlemm II, A. T. Y. Lui, G. Gloeckler, S. P. Christon, and F. Gliem, Geotail energetic particles and ion composition instrument, *J. Geomagn. Geoelectr.*, *46*, 39–57, 1994.

Wolf, R. A., The quasi-static (slow-flow) region of the magnetosphere, in *Solar-Terrestrial Physics*, edited by R. L. Carovillano and J. M. Forbes, p. 303, D. Reidel, Norwell, Mass., 1983.

L. Lyons and C.-P. Wang, Department of Atmospheric Sciences, University of California, Los Angeles, Los Angeles, CA 90095-1565, USA. (larry@atmos.ucla.edu; cat@atmos.ucla.edu)

T. Mukai and Y. Saito, Institute of Space and Astronautical Sciences, 3-1-1 Yoshinodai, Sagamihara, Kanagawa 229, Japan. (mukai@stp.isas.ac.jp; saito@stp.isas.ac.jp)

T. Nagai, Department of Earth and Planetary Sciences, Tokyo Institute of Technology, Ookayama 2-12-1, Meguro, Tokyo 152-8551, Japan. (nagai@geo.titech.ac.jp)

J. C. Samson, Department of Physics, University of Alberta, Edmonton, Alberta T6G 2E9, Canada. (samson@space.ualberta.ca)